Instruction for my personal numerical library

Tomohiro OISHI

26th March 2023

Abstract

This document is prepared to introduce and explain how to use the numerical library composed by T. OISHI. This library includes several source codes, whose final versions are expected to be published for some commercial purpose. Before the official publication, under the agreement with publishers, I make the current version open for public. Feedbacks and comments on products will be appreciated.

Acknowledgement

For composing this document as well as source codes in my library, the computer with Ubuntu LINUX and several free applications, including "gfortran", "gnuplot", "emacs", etc., are utilized. I am thankful for all the people, who had contributions to these products.

I would like to give my appreciation to the following people, who supported and supervised this work: Takeshi Yamamoto, Kazuhito Mizuyama, Takaaki Myo, Akira Ohnishi.

Contents

Chapter 1

Libra-01: TOSPEM

1.1 purpose

The code TOSPEM written in fortran-90 solves, for the spherical nucleus of (Z, N) protons and neutrons, (i) the Schroedinger equations for the single-nucleon states of the Woods-Saxon potential, (ii-a) the electric or magnetic transition strength, B_{EJ} or B_{MJ}, between the arbitrary set of initial and final states of the nucleus of interest, and (ii-b) Weisskopf estimate for comparison with results in (ii-a) [1]. The similar code was utilized in my past works [2, 3].

This note and the code TOSPEM are based on the CGS-Gauss system of units. The effective difference between the CGS-Gauss and SI (MKS-Ampere) systems is only for electro-magnetic quantities. See TABLE 1 for details.

1.2 structure of code

The code TOSPEM.f90 includes the following parts.

- "HONTAI" as the main part.
- "mdl_XXX_*" as the modules, including parameters, functions, and subroutines.
- "SPEM" for (i) solving the single-particle Schoedinger equation, and (ii) computing the B_{EJ} or B_{MJ} based on the formulas by Suhonen, Ring, and Schuck [4].
- "Weisskopf" for Weisskopf's estimate of B_{EJ} or B_{MJ}.
- There is the external file "PARAM.inp" for several input parameters. The quantum labels, $\{nlj\}$ for the initial and final states, and gyromagnetic factors, $g^{(p)}_{s/l}$ and $g^{(n)}_{s/l}$ for $M\lambda$ modes, are determined there.

Here the several TIPs for using this code.

- For compiling and excecuting the code, A_comprunshow.sh (shell-script file for BASH) is prepared.
- Cuoff parameters E_{cut}, l_{max}, R_{max}, and dr are fixed in the module, mdl_001_setting. If you change them, compile again the code.

- For determining the system of interest, fix these parameters: (i) zc and nc in mdl_001_setting; (ii) parameters r00, W_0, etc. in mdl_002_potentials. Also, modify the input parameters in "PARAM.inp" as necessary.
- In the module, mdl_002_potentials, single-particle potentials are determined as functions, v_cp and v_cn. Those are saved in output files, Yed_XXXX_SP_Potentials.dat.

1.3 single-nucleon states

In the first part of this code TOSPEM, the spherical Schroedinger equations are solved within the Woods-Saxon potential, which is determined in the fortran-90 module, MDL_002_POTENTIALS. The single-nucleon wave function satisfies

$$\psi_{nljm}(\boldsymbol{r}) = u_{nlj}(r)\mathcal{Y}_{ljm}(\bar{\boldsymbol{r}}), \tag{1.1}$$

where $\{n, l, j, m = -j \sim j\}$ indicate the radial node, orbital angular momentum, coupled angular momentum, and magnetic quantum number, respectively. Since spherical, what the code needs to compute is only the radial part $u_{nlj}(r)$. For example, the $0s_{1/2}$ state is solved as $u_{00\frac{1}{2}}(r)$. For numerical solution, the energy cutoff *ecut* and the radial box r_{max} are fixed in the module MDL_001_SETTING. Note also that each state is normalized in the code: $\int d\boldsymbol{r}\,|\psi_{nljm}(\boldsymbol{r})|^2 = 1$.

Here we discuss the example case of the spherical Schroedinger equation. That is

$$\left[-\frac{\hbar^2}{2\mu}\nabla^2_{\boldsymbol{r}} + V(r)\right]\psi(\boldsymbol{r}) = E\psi(\boldsymbol{r}). \tag{1.2}$$

The spherical solution generally reads

$$\psi_{nljm}(\boldsymbol{r}) = u_{nlj}(r)\mathcal{Y}_{ljm}(\bar{\boldsymbol{r}}) \equiv \frac{A(r)}{r}\mathcal{Y}_{ljm}(\bar{\boldsymbol{r}}), \tag{1.3}$$

Thus, by using $v(r) \equiv 2\mu V(r)/\hbar^2$ and $\epsilon \equiv 2\mu E/\hbar^2$, the equation changes as

$$\begin{aligned}\left[-\left(r^{-1}\frac{d^2}{dr^2}r - \frac{l(l+1)}{r^2}\right) + v(r) - \epsilon\right]\frac{A(r)}{r} &= 0 \\ \longrightarrow \left[\frac{d^2}{dr^2} - \frac{l(l+1)}{r^2} - v(r) + \epsilon\right]A(r) &= 0 \\ \frac{d^2}{dr^2}A(r) = G_E(r)A(r),&\end{aligned} \tag{1.4}$$

where

$$G_E(r) \equiv \frac{2\mu V(r)}{\hbar^2} + \frac{l(l+1)}{r^2} - \frac{2\mu E}{\hbar^2}. \tag{1.5}$$

Note also that

$$A(r \to 0) \cong r^{l+1}, \quad A'(r \to 0) \cong (l+1)r^{l+1},$$

as well as, when $V(r \to \infty) = 0$,

$$A(r \to \infty) \cong re^{-kr}, \quad A'(r \to \infty) \cong (1 - kr)e^{-kr},$$

where $k = \sqrt{-2\mu E}/\hbar$ for the bound state with $E < 0$. These asymptotic forms helf us to infer whether the numerical routine is correctly installed: if there is problem, the output wave functions do not behave like these asymptotic forms.

For the radial part, $u_{nlj}(r) = \frac{A_{nlj}(r)}{r}$, where the function $A_{nlj}(r)$ is computed with "Numerov method" [5]. The radial equation reads

$$\left[\frac{d^2}{dr^2} + w(r)\right] A(r) = 0, \tag{1.6}$$

after some reformulation. Then, if one can determine the first two points, $A_0 \equiv A(r_0)$ and $A_1 \equiv A(r_1)$ from e.g. the asymptotic form, the remaining points are computed as

$$A_{n+1} \cong \frac{(2 - 5a^2 w_n/6)A_n - (1 + a^2 w_{n-1})A_{n-1}}{1 + a^2 w_{n+1}/12}, \tag{1.7}$$

where a is the radial mesh. For details on Numerov method, see Appendix B.

In the code, there are two subroutines of Numerov methods starting from $r = 0$ fm and $r = r_{max}$. The matching of these two solutions is necessary in order to correctly find the eigenenergies and node numbers for bound states.

1.4 sample calcuation of single-nucleon states

Here I introduce the results of sample calculations for the ^{40}Ca nucleus. In the code, each energy level is solved by matching the forward and backward Numerov solutions. Then, radial-wave functions, $A_{nlj}(r) \equiv r \cdot u_{nlj}(r)$, are stored as the array "psi". Those are normalized as $\int dr r^2 \left|u_{nlj}(r)\right|^2 = \int dr \left|A_{nlj}(r)\right|^2 = 1$.

1.4.1 neutron states

The single-particle Schrödinger equation for neutrons is given as

$$\left[-\frac{\hbar^2}{2\mu}\nabla_{\boldsymbol{r}}^2 + V(r)\right]\psi(\boldsymbol{r}) = E\psi(\boldsymbol{r}), \tag{1.8}$$

where $\mu = m_n m_c/(m_n + m_c)$, $m_c = 20m_n + 20m_p - 40B/c^2$, $m_n c^2 = 939.5654133$ MeV, $m_p c^2 = 938.2720813$ MeV, and $B = 8.551305$ MeV, which is the binding energy per nucleon of ^{40}Ca [6]. The Woods-Saxon potential reads

$$\begin{aligned} V(r) &= V_{WS}(r) = V_0 f(r) + U_{ls}(\boldsymbol{l}\cdot\boldsymbol{s})\frac{1}{r}\frac{df(r)}{dr}, \\ f(r) &= \frac{1}{1 + e^{(r-R_0)/a_0}}, \end{aligned} \tag{1.9}$$

where $R_0 = r_0 \cdot 40^{1/3}$, and $f(r)$ is the standard Fermi profile. In this library, I fix the parameters as $V_0 = -55.57$ MeV, $U_{ls} = 11.28$ MeV·fm^2, $r_0 = 1.25$ fm, and $a_0 = 0.65$ fm. In addition, I employ the cutoff parameters, $r_{max} = 30$ fm, $dr = 0.1$ fm, $l_{max} = 5$, and $E_{max} = 18$ MeV. The results are obtained as follows.

```
(neutron-core) s.p. states
   # Node     L     J*2       E(MeV)
   1    0     0     1     -42.6596966
   2    0     1     3     -32.0630613
   3    0     1     1     -31.2326299
   4    0     2     5     -20.4627846
```

```
    5     0     2     3     -18.7572561
    6     1     0     1     -17.7700038
    7     0     3     7      -8.3626685
    8     1     1     3      -6.2390782
    9     0     3     5      -5.7572462
   10     1     1     1      -5.4529772
   11     2     0     1       0.1683648
   12     2     1     3       0.5043552
   13     2     1     1       0.5071959
   14     1     2     5       0.7622601
   15     1     2     3       0.7713305
   16     3     0     1       0.8443721
   17     1     3     7       1.1522559
   18     1     3     5       1.1525952
   19     3     1     3       1.5695544
   20     0     4     9       1.5799132
   89     8     2     3      17.8490518
number of s.p.basis=           89
```

1.4.2 proton states

For proton states, the single-particle Schrödinger equation should include the repulsive Coulomb potential. In this library, the potential of uniformly-charged spherical core is employed. Namely,

$$V(r) = V_{WS}(r) + V_C(r), \qquad V_C(r) = \begin{cases} \frac{Ze^2}{r} & (r \geq R_0), \\ \frac{Ze^2}{2R_0}\left[3 - \left(\frac{r}{R_0}\right)^2\right] & (r < R_0), \end{cases} \tag{1.10}$$

with $R_0 = r_0 \cdot 40^{1/3}$. Also the relative mass should be slightly modified as $\mu = m_p m_c/(m_p + m_c)$. Then the results are obtained as follows. Notice that each proton's energy is higher than the neutron's energy, because of the repulsive Coulomb potential. Several levels become unbound in the proton side.

```
(proton-core) s.p. states
   # Node     L     J*2       E(MeV)
    1     0     0     1     -33.6446148
    2     0     1     3     -23.5993700
    3     0     1     1     -22.7430551
    4     0     2     5     -12.5323720
    5     0     2     3     -10.7995723
    6     1     0     1      -9.8024169
    7     0     3     7      -1.0297129
    8     1     1     3       0.6845982
    9     1     1     1       1.3588870
   10     0     3     5       1.5319337
   11     2     0     1       1.9225865
   12     2     1     3       2.0435195
   13     2     1     1       2.0490777
   14     1     2     5       2.2519461
   15     1     2     3       2.2520630
   16     1     3     7       2.5540474
   17     1     3     5       2.5543557
   18     0     4     9       2.9317977
   19     0     4     7       2.9318078
   20     3     0     1       3.2036884
```

```
   80     5     5    11      17.7374567
 number of s.p.basis=           80
```

1.5 electic/magnetic transitions

Electro-magnetic multipole transition of single nucleon inside atomic nuclei is described by the operator,

$$\hat{\mathcal{Q}} = \hat{\mathcal{Q}}(X\lambda\mu, \boldsymbol{r}_{p/n}), \tag{1.11}$$

where $X = E$ (M) for the electric (magnetic) mode. Its formalism is given as Eqs. (B.23) and (B.24) in the textbook [7]. Those are,

$$\begin{aligned}
\hat{\mathcal{Q}}(E\lambda\mu, \boldsymbol{r}) &= e_{\rm eff} r^\lambda Y_{\lambda\mu}(\bar{\boldsymbol{r}}), \\
\hat{\mathcal{Q}}(M\lambda\mu, \boldsymbol{r}) &= \mu_{\rm N} \left(\vec{\nabla} r^\lambda Y_{\lambda\mu}(\bar{\boldsymbol{r}})\right) \cdot \left(\frac{2g_l}{\lambda+1}\hat{\boldsymbol{l}} + g_s \hat{\boldsymbol{s}}\right),
\end{aligned}$$

where $e_{\rm eff}$, $\mu_{\rm N}$ (nuclear magneton), g_l, and g_s are the well-known effective parameters [7, 8]. Usually, for the proton (neutron), $e_{\rm eff} = {\rm e}$ (0), $g_l = 1$ (0), and $g_s = 5.586$ (-3.826). Also, the nuclear magneton is given as $\mu_{\rm N} = {\rm e}\hbar/2m_p c \cong 0.10515\,[{\rm e}\cdot{\rm fm}]$.

Transition probability per time is given as Eq. (B.72) in Ref. [7]:

$$\begin{aligned}
T(X\lambda\mu; i\to f) &= \frac{8\pi}{\hbar} f(\lambda) \left(\frac{E_{fi}}{\hbar c}\right)^{2\lambda+1} \times B(X\lambda\mu; i\to f) \quad [s^{-1}], \text{ with} \\
f(\lambda) &\equiv \frac{\lambda+1}{\lambda} \frac{1}{[(2\lambda+1)!!]^2},
\end{aligned} \tag{1.12}$$

where $E_{fi} = E_f - E_i$ [1]. Here $B(i\to f)$ is the total transition strength, which is represented as

$$B(X\lambda\mu; i\to f) = \frac{1}{2I_i+1} \sum_{\mu M_i M_f} \left| \left\langle I_f M_f \left| \hat{\mathcal{Q}}(X\lambda\mu) \right| I_i M_i \right\rangle \right|^2. \tag{1.13}$$

Note that its unit is commonly $[{\rm e}^2\cdot({\rm fm})^{2\lambda}]$. If both the inital and final states are spherical, this can be reduced as

$$B(X\lambda\mu; j_i\to j_f) = \frac{1}{2j_i+1} \left| \left\langle j_f \left\| \hat{\mathcal{Q}}(X\lambda) \right\| j_i \right\rangle \right|^2, \tag{1.14}$$

by Wigner-Eckart theorem. In the code TOSPEM, these reduced amplitudes are computed according to Eq.(B.81) and Eq.(B.82) in Ref. [7]. Namely, for electric modes,

$$\begin{aligned}
\left\langle j_f \left\| \hat{\mathcal{Q}}(EJ) \right\| j_i \right\rangle &= {\rm e}\frac{1+(-)^{j_i+j_f+J}}{2} \left\langle u_f \mid r^J \mid u_i \right\rangle \\
&\quad w(J, j_f, j_i)(-)^{j_f-1/2} \begin{pmatrix} j_f & J & j_i \\ -\frac{1}{2} & 0 & \frac{1}{2} \end{pmatrix},
\end{aligned} \tag{1.15}$$

where

$$w(J, j_f, j_i) \equiv \sqrt{\frac{(2J+1)(2j_i+1)(2j_f+1)}{4\pi}}. \tag{1.16}$$

[1] Within the MKS-Ampere system of units, the first factor of Eq.(1.12) should be replaced into $\frac{2}{\epsilon_0\hbar}$. Note also that the definition of $\mu_{\rm N}$ should be different from that in the CGS-Gauss system.

For magnetic modes, on the other side,

$$\left\langle j_f \left\| \hat{\mathcal{Q}}(MJ) \right\| j_i \right\rangle = \mu_{\rm N} \frac{1-(-)^{j_i+j_f+J}}{2} \left\langle u_f \mid r^{J-1} \mid u_i \right\rangle \\ w(J, j_f, j_i)(-)^{j_f-1/2} \begin{pmatrix} j_f & J & j_i \\ -\frac{1}{2} & 0 & \frac{1}{2} \end{pmatrix} \\ (J-k)\left(\frac{g_s}{2} - g_l - g_l \frac{k}{J+1}\right), \tag{1.17}$$

with

$$k \equiv \left(j_f + \frac{1}{2}\right)(-)^{l_f+j_f+\frac{1}{2}} + \left(j_i + \frac{1}{2}\right)(-)^{l_i+j_i+\frac{1}{2}}. \tag{1.18}$$

Note that the radial integration,

$$\left\langle u_f \mid r^N \mid u_i \right\rangle = \int r^2 dr \; u_{n_f,l_j,j_f}(r) r^N u_{n_i,l_i,j_i}(r), \tag{1.19}$$

is numerically computed in the subroutine "SPEM". On the other side, this radial integration is approximated in the Weisskopf's estimate [1].

Table 1: Notations in the SI (MKS-Ampere) and CGS-Gauss systems of units especially for nuclear-physical quantities [7, 8]. Note also that $m_p \cong 938.272$ MeV/c^2 (proton mass), and fm^2 = 10 mb= 10^{-2} barn for the typical order of cross sections.

Quantity	SI [unit]	CGS-Gauss [unit]	Note
Elementary charge	$\equiv e$	$\equiv$ e	convertion:
	$\cong 1.602 \times 10^{-19}$[C]		$e^2 \longrightarrow 4\pi\epsilon_0 \mathrm{e}^2$
Coulomb potential	$V = \frac{1}{4\pi\epsilon_0}\frac{e^2}{r}$ [MeV]	$= \frac{\mathrm{e}^2}{r}$ [MeV]	between 2p
Fine-structure constant	$\alpha = \frac{e^2}{4\pi\epsilon_0\hbar c}$	$= \frac{\mathrm{e}^2}{\hbar c}$	$\cong \frac{1}{137.036}$
Nuclear magneton	$\mu_{\rm N} = \frac{e\hbar}{2m_p}$	$\mu_{\rm N} = \frac{\mathrm{e}\hbar}{2m_p c}$	
	$\cong 0.10515$ [ce·fm]	$\cong 0.10515$ [e·fm]	
$B_{EJ}(E)$	in $\left[e^2\mathrm{fm}^{2J}\right]$	in $\left[\mathrm{e}^2\mathrm{fm}^{2J}\right]$	
$B_{MJ}(E)$	in $\left[\frac{\mu_{\rm N}^2}{c^2}\mathrm{fm}^{2J-2}\right]$	in $[\mu_{\rm N}^2\mathrm{fm}^{2J-2}]$	
	$\cong 1.106 \times 10^{-2}\left[e^2\mathrm{fm}^{2J}\right]$	$\cong 1.106 \times 10^{-2}\left[\mathrm{e}^2\mathrm{fm}^{2J}\right]$	
$T_{EJ/MJ}(E)$	$= \frac{2}{\epsilon_0\hbar} f(J)\left(\frac{E}{\hbar c}\right)^{2J+1}$	$= \frac{8\pi}{\hbar} f(J)\left(\frac{E}{\hbar c}\right)^{2J+1}$	$f(J) \equiv \frac{J+1}{J}$
	$\times B_{EJ/MJ}(E)$	$\times B_{EJ/MJ}(E)$	$\times \left(\frac{1}{(2J+1)!!}\right)^2$

1.5.1 Weisskopf estimate

In paper [1], Weisskopf presented an estimate generally for EJ and MJ transitions of the single proton inside nuclei. From Weisskopf's estimate [1,7], one can infer that, for the electric mode,

$$B_p(E\lambda\mu; I_i \to I_f) \cong \frac{1}{4\pi}\left(\frac{3}{\lambda+3}\right)^2 \left(1.21A^{1/3}\right)^{2\lambda} \quad \left[e^2(\mathrm{fm})^{2\lambda}\right]. \tag{1.20}$$

For the magnetic mode, by using an approximation as $\left(\frac{g_s^{(p)}}{2}\right)^2 + 1 \cong 10$ for proton's spin-gyromagnetic factor,

$$B_p(M\lambda\mu; I_i \to I_f) \cong \frac{10}{\pi}\left(\frac{3}{\lambda+3}\right)^2 \left(1.21A^{1/3}\right)^{2\lambda-2} \quad [\mu_\mathrm{N}^2(\mathrm{fm})^{2\lambda-2}], \tag{1.21}$$

where $\mu_\mathrm{N}^2 \cong 1.106 \times 10^{-2}$ [e^{2}fm^2]. In this library, instead of Weisskopf's original setting, an approximation of $\left(\frac{g_s^{(p)}}{2}\right)^2 + 1 \cong 8.8$ for proton's spin-gyromagnetic factor is employed.

Pay attention on that, in the neutron case, this estimate cannot apply directly, because (i) its electric charge is zero, and (ii) gyromagnetic factor is different from proton's one. In this library, I assume that (i) the neutron has the imaginary electric charge $+e$, as well as (ii) $g_s^{(n)} = -3.862$ and $g_l^{(n)} = 0$.

1.6 sample calcuation of electric/magnetic transitions

With the same setting and parameters in section 1.4, by using the wave functions solved there, the results of sample calculations for the ^{40}Ca nucleus are presented. The $E1$ and $M1$ transitions are computed. In the code TOSPEM.f90, three method are compared. Namely, (A) full computation [7], (B) Weisskopf estimate, and (C) as the same to (A), but the radial integration of $B(EJ/MJ)$ is replaced to that in the method (B).

1.6.1 E1 transitions

$E1$ transitions of $0d_{3/2} \longrightarrow 1s_{1/2}$. For the proton, $B_p(E1) = 0.236$ e^{2}fm^2 in (A), and 0.754 e^{2}fm^2 in (B)=(C). For the neutron, $B_n(E1) = 0.235$ e^{2}fm^2 in (A), and 0.754 e^{2}fm^2 in (B)=(C). Note that here I assumed that the neutron has the charge of +e commonly to the proton. The output appears as follows.

```
 Mode of Q(J):           8 for (8:Elec, 9:Mag) with J =          1
  |i>   with (n,l,j*2)=  0       2       3
    <f| with (n,l,j*2)=  1       1       1  (proton)
  |i>   with (n,l,j*2)=     0       2       3
    <f| with (n,l,j*2)=     1       1       1  (neutron)
 <><<><><><><<><><><><<><><><><<><><><><<><><><><<><><><><<><><><>
  [A] Suhonen's formulas Eq. (6.23) and (6.24), where
      both the radial and angular integrations are properly computed:
-->   B_{QJ} =|<f|Q(J)|i>|**2 /(2j_i +1) =       0.236420 (proton)
-->                                            0.235329 (neutron)
  ---
  radial integration of <f|Q|i> =   -1.7236413891321813       (prot.)
                                =   -1.7196615102431740       (neut.)
  ---
```

```
  angular part of <f|Q_J|i> =  0.56418958360071603   (prot.)
                            =  0.56418958360071603   (neut.)
 <><<><><><<><><><><<><><><<><><<><><><><<><><><<><><><<><><<><><>
  [B] VS Weisskopf estimate (1) [Phys. Rev. (1951) 83, 1073]:
  Mode of Q(J):   8 for (8:Elec, 9:Mag) with J =          1
-->    B_{QJ} =|<f|Q(J)|i>|**2 /(2j_i +1) =       0.753902 (proton)
-->                                               0.753902 (neutron)
  Same but without A-dep. factor f_J =x^{J}   for EJ mode,
    where x=A^{2/3},        or   f_J =x^{J-1} for MJ mode:
-->           B_{QJ} /f_J      =       0.064458 (proton)
-->                                   0.064458 (neutron)
 <><<><><><<><><><><<><><><<><><<><><><><<><><><<><><><<><><<><><>
  [C] VS Weisskopf estimate (2), where
  radial integration is approximated as ~= (3*R**N)/(3 + ilam),
  where R=1.2*ac**(1/3) and N=ilam (ilam-1) for E (M),
  whereas the angular part is computed commonly as in [A]:
-->   B_{QJ} =|<f|Q(J)|i>|**2 /(2j_i +1) =       0.753902 (proton)
-->                                              0.753902 (neutron)
  angular part of <f|Q|i> =  0.564189583600 (prot.)
                          =  0.564189583600 (neut.)
  ---
  radial part of <f|Q|i>, approximated as
  ~= (3*R**N)/(3 + ilam) =   3.07795670   (prot.)
                         =   3.07795670   (neut.)
```

Notice that the radial integration of $B(E1)$ is over estimated in (B) and (C) by Weisskopf.

1.6.2 M1 transitions

$M1$ transitions of $0f_{7/2} \longrightarrow 0f_{5/2}$. For the proton, $B_p(M1) = 2.145\ \mu_{\rm N}^2$ in (A), 1.576 $\mu_{\rm N}^2$ in (B), and 1.210 $\mu_{\rm N}^2$ in (C). For the neutron, $B_n(M1) = 1.496\ \mu_{\rm N}^2$ in (A), 0.655 $\mu_{\rm N}^2$ in (B), and 0.842 $\mu_{\rm N}^2$ in (C). Note that g factors are different between protons and neutrons.

Chapter 2

Libra-02: RESONA

On 2023/March/09th, I had started to buid up the library of solvers for the resonant eigenstates of Schoedinger equations. Then, the four different solvers, (i) the graphic fitting of energy stabilization, (ii) time-dependent (TD) calculation, (iii) scattering phase-shift calculation, and (iv) complex scaling method were implemented. Consistency between these methods were confirmed for the resonance problem of ^{16}O+$n(d_{3/2})$.

2.1 parameters for testing calculations

For this library, a spherical Schoedinger equation is solved for benchmark. That reads

$$\left[-\frac{\hbar^2}{2\mu}\frac{d^2}{dr^2}+\frac{\hbar^2}{2\mu}\frac{l(l+1)}{r^2}+V(r)\right]\psi(r)=\epsilon\psi(r), \tag{2.1}$$

where $\epsilon = E - i\Gamma/2$. I assume the ^{16}O+n system, and thus, $\mu = m_n m_c/(m_n + m_c)$, where m_c (m_n) is the core-nucleus (neutron) mass. The single-particle potential $V(r)$ is determined as the Woods-Saxon plus spin-orbit potential. That is given as

$$\begin{aligned} V(r) &= V_{WS}(r) = V_0 f(r) + U_{ls}(\boldsymbol{l}\cdot\boldsymbol{s})\frac{1}{r}\frac{df(r)}{dr}, \\ f(r) &= \frac{1}{1+e^{(r-R_0)/a_0}}, \end{aligned} \tag{2.2}$$

where $R_0 = r_0 \cdot A_{core}^{1/3} = r_0 \cdot 16^{1/3}$, and $f(r)$ is the standard Fermi profile. In this library, I fix the parameters as $V_0 = -53.2$ MeV, $U_{ls} = 22.1$ MeV·fm^2, $r_0 = 1.25$ fm, and $a_0 = 0.65$ fm. Note also that, if the particle was proton, the Coulomb potential $V_{Coul}(r)$ of an uniformly charged sphere with radius R_0 should be employed for the core-proton potential: $V(r) = V_{WS}(r) + V_{Coul}(r)$.

The potential (2.2) has the single-neutron bound states with $E_n(0s_{1/2}) = -31.970$ MeV, $(0p_{3/2}) = -17.846$ MeV, $(0p_{1/2}) = -14.594$ MeV, $(0d_{5/2}) = -4.143$ MeV, and $(1s_{1/2}) = -3.275$ MeV. Then, in the $0d_{3/2}$ channel, the first resonant state could exist. Note that this neutron resonance appears in some excited state, not in the ground state.

2.2 scattering phase-shift calculation

Result: $E = 415.5$ keV, $\Gamma = 16.6$ keV, for ^{16}O+$n(0d_{3/2})$.

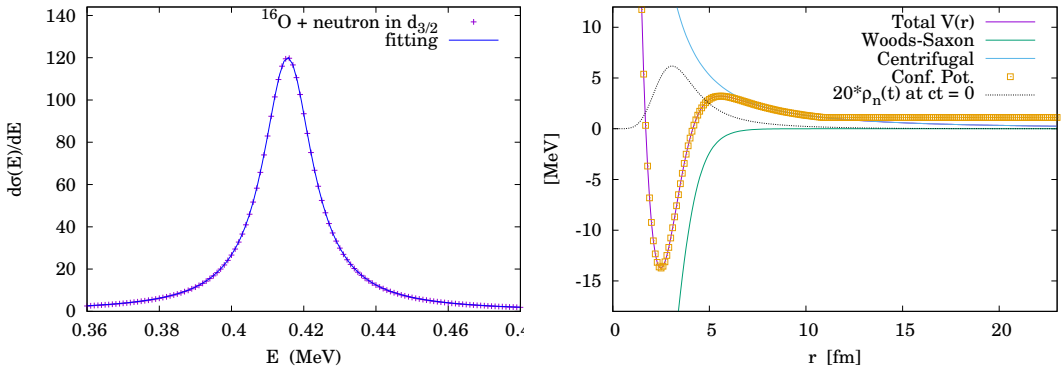

Figure 2.1: caption.

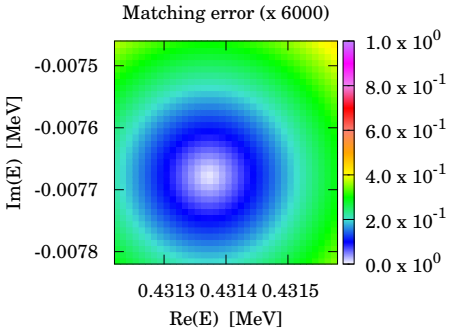

Figure 2.2: caption.

Details of phase-shift calculations are summarized in Appendix C. The phase shift of scattering problem of Eq. (2.1) is computed within the code "SCPSTD.f90", which is the same code for the TD calculations. Figure 2.1 shows the phase-shift $\sigma(E)$ calculated in the $d_{3/2}$ ($l = 2,\ j = 3/2$) channel. There, the obtained $d\sigma/dE$ distribution is fitted by a Breit-Wigner profile. As the result, this ^{16}O+n system with the potential given in Eq. (2.2) has one resonant state in the $d_{3/2}$ channel at $E = 415.5$ keV with the width $\Gamma = 16.6$ keV.

In the source code "SCPSTD.f90", for computing the phase shift, the open-source code "COULCC" by Thompson and Barnett is copied and utilized [9].

2.3 time-dependent method

Result: $E = 428.5$ keV, $\Gamma = 16.7$ keV, for ^{16}O+$n(0d_{3/2})$.

Figure 2.1 shows the core-neutron potential in the $d_{3/2}$ ($l = 2,\ j = 3/2$) channel. Notice that the total potential $V(r)$ has a barrier as obtained from the Woods-Saxon and centrifugal potentials. The time-dependent (TD) calculation is perfomred from the initial state, where the wave packet is well confined inside this barrier. As the result, the $1n$-emission width is obtained as $\Gamma \cong 16.7$ keV with the Q value, $E = Q_{1n} \cong 421.8$ keV.

The code "SCPSTD.f90" is utilized for TD calculations. This code solves Eq. (2.1) with the Numerov method, where its details are summarized in Appendix B. The initial state is determined within the confining potential as shown in Fig. 2.1.

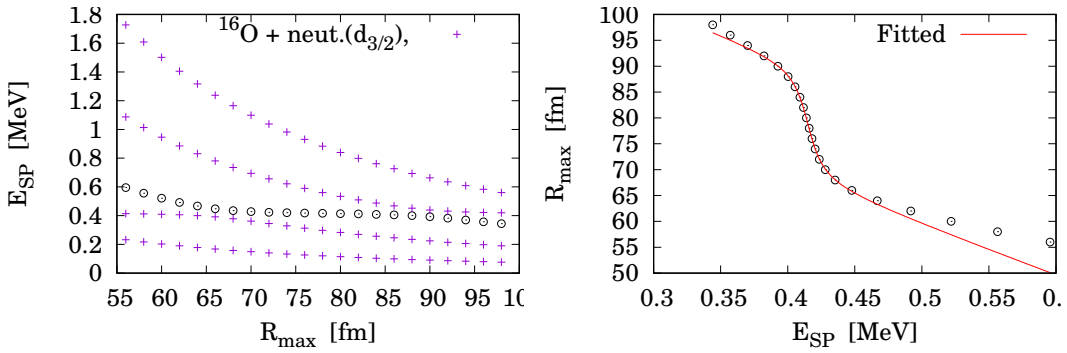

Figure 2.3: caption.

2.4 complex-scaling method

Result: $E = 431.4$ keV, $\Gamma = 15.4$ keV, for ^{16}O+$n(0d_{3/2})$.

Complex-scaled Runge-Kutta (CSRK4) method is utilized to obtain the complex eigenenergy of Eq. (2.1). See Appendix A for details on the Runge-Kutta method. The error of matching is displayed in Fig. 2.2.

2.5 energy stabilization method

Result: $E = 415.1$ keV, $\Gamma = 16.7$ keV, for ^{16}O+$n(0d_{3/2})$.

For computing the eigenenergies above threshold by changing r_{max}, I compose the shell-script file, "Sequence_v2.sh", as following.

```
#!/bin/sh
l=3000000
n=560
z=20
rm  OUTRU*.txt  Rmax_and_En*.txt
while [ $n -ne 1000 ]
do
  echo "(N=${n})-operation"
  sed "4 s/=.../=$n/" SCPSTD.f90 > Main.f90
  gfortran  Main.f90  -o  run.out
  b=`expr $n + $l`
  time ./run.out > OUTRUN_${b}.txt
  mv  Rmax_and_Energies.txt  Rmax_and_Enes_${b}.txt
  n=`expr $n + $z`
  echo "------------------------------------------------------------"
done
#grep  "fm, MeV"  ./Rmax*.txt  >  Dummy.dat
#sed  "s/..Rmax_and_Enes_.....txt:/ /"  Dummy.dat  >  Fine.dat
cat  Rmax_and_Enes_*.txt  >  Fine.dat
```

Here the original f90 file, "SCPSTD.f90", includes the sentences,

```
module mdl_001_setting                                          !L0002
   implicit none                                                !L0003
   integer, parameter :: nrmax =xxx                             !L0004
   double precision, parameter :: dr = 0.1d0                    !L0005
```

```
   double precision, parameter :: rmax = dr*(dble(nrmax) +1.d-11)      !L0006
```

where the 4th line is modified in each iteration.

Chapter 3

Samples for documentation

This is the place to store copy-and-paste materials.

3.1 sample of matrix-form equation

In this library, the potential of uniformly-charged spherical core is employed. Namely,

$$V(r) = V_{WS}(r) + V_C(r), \quad V_C(r) = \begin{cases} \frac{Ze^2}{r} & (r \geq R_0), \\ \frac{Ze^2}{2R_0}\left[3 - \left(\frac{r}{R_0}\right)^2\right] & (r < R_0), \end{cases} \tag{3.1}$$

with $R_0 = r_0 \cdot 40^{1/3}$.

By using $B(r) \equiv \frac{dA}{dr}$, Eq.(A.3) becomes

$$\frac{dA}{dr} = B(r), \quad \frac{dB}{dr} = G_E(r)A(r). \tag{3.2}$$

Or equivalently,

$$\frac{d}{dr}\begin{pmatrix} A(r) \\ B(r) \end{pmatrix} = \begin{pmatrix} 0 & 1 \\ G_E(r) & 0 \end{pmatrix}\begin{pmatrix} A(r) \\ B(r) \end{pmatrix}. \tag{3.3}$$

This equation can be solved with e.g. Runge-Kutta method. Note also that

$$\begin{aligned} A(r \to 0) &\cong r^{l+1}, \\ A'(r \to 0) &\cong (l+1)r^{l+1}, \end{aligned} \tag{3.4}$$

as well as, when $V(r \to \infty) = 0$,

$$\begin{aligned} A(r \to \infty) &\cong re^{-kr}, \\ A'(r \to \infty) &\cong (1 - kr)e^{-kr}, \end{aligned} \tag{3.5}$$

where $k = \sqrt{-2\mu E}/\hbar$ for the bound state with $E < 0$. These asymptotic forms helf us to infer whether the numerical routine is correctly installed: if there is problem, the output wave functions do not behave like these asymptotic forms.

3.2 sample of displaying code

In the following, we describe some examples. For this purpose, we employ the software *gnuplot* and its script as follows.

```
# (d/dt) n1(t) = -b * n2(t)
# (d/dt) n2(t) = -c * n1(t)

#--- Input-1: initial numbers of soldiers (powers). Default=(a)
n1_0 = 5.0 ; n2_0 = 3.0

#--- Input-2: proficiency factors, (b,c). Default=(a)
p = 1.0
b = 1.0*p ; c = 1.0*p
#b = p*(n1_0/n2_0)**2 ; c = p ### factors for "never-ending combat".

#--- Results:
a = sqrt(b*c) ; d = sqrt(b/c)

f0   = (n1_0 + d*n2_0) * 0.5 ; g0   = (n1_0 - d*n2_0) * 0.5
f(x) = f0 * exp(-a*x)              ; g(x) = g0 * exp( a*x)

w1 = -0.5*log( g0/f0) / a ### Time when "n_2(w1)=0".
#w2 = -0.5*log(-g0/f0) / a ### Time when "n_1(w2)=0".

n1(x) =  f(x) + g(x)
n2(x) = (f(x) - g(x)) / d
s(x) = n1(x)-n2(x)
t(x) = n1(w1)
z(x) = 0
```

Dummy text. Dummy text.

3.3 sample of TABLE

Here several examples of TABLE are presented.

Table 1: (Example of TABLE).

	^{37}Sc		^{39}Sc	
	Q_p	Γ_p	Q_p	Γ_p
DD-PCX + D1S Pair.	2.72	3.74×10^{-3}	0.662	3.87×10^{-9}
		$(\tau = 1.76 \times 10^{-19}$ s)		$(\tau = 1.70 \times 10^{-13}$ s)
Experimental Data [6]	2.9 ± 0.3	–	0.597 ± 0.024	$(\tau < 400$ ns)

Dummy text. Dummy text.

Table 2: Notations in the SI (MKS-Ampere) and CGS-Gauss systems of units especially for nuclear-physical quantities [7, 8]. Note also that $m_p \cong 938.272$ MeV/c^2 (proton mass), and $\mathrm{fm}^2 = 10$ mb$= 10^{-2}$ barn for the typical order of cross sections.

Quantity	SI [unit]	CGS-Gauss [unit]	Note
Elementary charge	$\equiv e$	$\equiv \mathrm{e}$	convertion:
	$\cong 1.602 \times 10^{-19}$[C]		$e^2 \longrightarrow 4\pi\epsilon_0 \mathrm{e}^2$
Coulomb potential	$V = \frac{1}{4\pi\epsilon_0}\frac{e^2}{r}$ [MeV]	$= \frac{\mathrm{e}^2}{r}$ [MeV]	between 2p
Fine-structure constant	$\alpha = \frac{e^2}{4\pi\epsilon_0\hbar c}$	$= \frac{\mathrm{e}^2}{\hbar c}$	$\cong \frac{1}{137.036}$
Nuclear magneton	$\mu_\mathrm{N} = \frac{e\hbar}{2m_p}$	$\mu_\mathrm{N} = \frac{\mathrm{e}\hbar}{2m_p c}$	
	$\cong 0.10515$ [ce·fm]	$\cong 0.10515$ [e·fm]	
$B_{EJ}(E)$	in $\left[e^2\mathrm{fm}^{2J}\right]$	in $\left[\mathrm{e}^2\mathrm{fm}^{2J}\right]$	
$B_{MJ}(E)$	in $\left[\frac{\mu_\mathrm{N}^2}{c^2}\mathrm{fm}^{2J-2}\right]$	in $[\mu_\mathrm{N}^2\mathrm{fm}^{2J-2}]$	
	$\cong 1.106 \times 10^{-2}\left[e^2\mathrm{fm}^{2J}\right]$	$\cong 1.106 \times 10^{-2}\left[\mathrm{e}^2\mathrm{fm}^{2J}\right]$	
$T_{EJ/MJ}(E)$	$= \frac{2}{\epsilon_0\hbar} f(J)\left(\frac{E}{\hbar c}\right)^{2J+1}$	$= \frac{8\pi}{\hbar} f(J)\left(\frac{E}{\hbar c}\right)^{2J+1}$	$f(J) \equiv \frac{J+1}{J}$
	$\times B_{EJ/MJ}(E)$	$\times B_{EJ/MJ}(E)$	$\times \left(\frac{1}{(2J+1)!!}\right)^2$

Appendix A

Runge-Kutta method

The code CSTEST.F90 written in fortran-90 solves, for the spherical Schroedinger (Dirac) equation, not only the bound but also resonant states with complex-scaling (CS) method. This note and the code CSTEST.F90 are based on the SI system of units.

A.1 radial wave functions

Here we discuss the spherical Schroedinger equation. That is

$$\left[-\frac{\hbar^2}{2\mu}\nabla_{\boldsymbol{r}}^2 + V(r)\right]\psi(\boldsymbol{r}) = E\psi(\boldsymbol{r}). \tag{A.1}$$

The spherical solution generally reads

$$\psi(\boldsymbol{r}) = \frac{A(r)}{r}Y_{lm}(\theta,\phi). \tag{A.2}$$

Thus, by using $v(r) \equiv 2\mu V(r)/\hbar^2$ and $\epsilon \equiv 2\mu E/\hbar^2$, the equation changes as

$$\begin{aligned}\left[-\left(r^{-1}\frac{d^2}{dr^2}r - \frac{l(l+1)}{r^2}\right) + v(r) - \epsilon\right]\frac{A(r)}{r} &= 0 \\ \longrightarrow \left[\frac{d^2}{dr^2} - \frac{l(l+1)}{r^2} - v(r) + \epsilon\right]A(r) &= 0 \\ \frac{d^2}{dr^2}A(r) = G_E(r)A(r), &\end{aligned} \tag{A.3}$$

where

$$G_E(r) \equiv \frac{2\mu V(r)}{\hbar^2} + \frac{l(l+1)}{r^2} - \frac{2\mu E}{\hbar^2}. \tag{A.4}$$

By using $B(r) \equiv \frac{dA}{dr}$, Eq.(A.3) becomes

$$\frac{dA}{dr} = B(r), \qquad \frac{dB}{dr} = G_E(r)A(r). \tag{A.5}$$

Or equivalently,

$$\frac{d}{dr}\begin{pmatrix} A(r) \\ B(r) \end{pmatrix} = \begin{pmatrix} 0 & 1 \\ G_E(r) & 0 \end{pmatrix}\begin{pmatrix} A(r) \\ B(r) \end{pmatrix}. \tag{A.6}$$

This equation can be solved with e.g. Runge-Kutta method. Note also that

$$\begin{aligned} A(r \to 0) &\cong r^{l+1}, \\ A'(r \to 0) &\cong (l+1) r^{l+1}, \end{aligned} \tag{A.7}$$

as well as, when $V(r \to \infty) = 0$,

$$\begin{aligned} A(r \to \infty) &\cong r e^{-kr}, \\ A'(r \to \infty) &\cong (1 - kr) e^{-kr}, \end{aligned} \tag{A.8}$$

where $k = \sqrt{-2\mu E}/\hbar$ for the bound state with $E < 0$. These asymptotic forms helf us to infer whether the numerical routine is correctly installed: if there is problem, the output wave functions do not behave like these asymptotic forms.

A.2 implementation of Runge-Kutta method

Equation of interest here is given as

$$\frac{d}{dr} \begin{pmatrix} A(r) \\ B(r) \end{pmatrix} = \begin{pmatrix} a(r) & b(r) \\ c(r) & d(r) \end{pmatrix} \begin{pmatrix} A(r) \\ B(r) \end{pmatrix}. \tag{A.9}$$

We assume that $A_0 = A(r_0)$ and $B_0 = B(r_0)$ are already known. Runge-Kutta method gives the numerical solution in the mesh points $r_{n+1} = r_n + D$ as [10]

$$\begin{aligned} A_{n+1} &= A_n + \frac{D}{6}\left(u_1 + 2u_2 + 2u_3 + u_4\right), \\ B_{n+1} &= B_n + \frac{D}{6}\left(v_1 + 2v_2 + 2v_3 + v_4\right). \end{aligned} \tag{A.10}$$

Here the 1st to 4th-step elements read

$$\begin{aligned} u_1 &= \left[a(s_1)A_n + b(s_1)B_n\right], \\ u_2 &= \left[a(s_2)\left(A_n + \frac{D}{2}u_1\right) + b(s_2)\left(B_n + \frac{D}{2}v_1\right)\right], \\ u_3 &= \left[a(s_3)\left(A_n + \frac{D}{2}u_2\right) + b(s_3)\left(B_n + \frac{D}{2}v_2\right)\right], \\ u_4 &= \left[a(s_4)\left(A_n + Du_3\right) + b(s_4)\left(B_n + Dv_3\right)\right], \end{aligned} \tag{A.11}$$

and

$$\begin{aligned} v_1 &= \left[c(s_1)A_n + d(s_1)B_n\right], \\ v_2 &= \left[c(s_2)\left(A_n + \frac{D}{2}u_1\right) + d(s_2)\left(B_n + \frac{D}{2}v_1\right)\right], \\ v_3 &= \left[c(s_3)\left(A_n + \frac{D}{2}u_2\right) + d(s_3)\left(B_n + \frac{D}{2}v_2\right)\right], \\ v_4 &= \left[c(s_4)\left(A_n + Du_3\right) + d(s_4)\left(B_n + Dv_3\right)\right], \end{aligned} \tag{A.12}$$

within the coordinates, $s_1 = r_n$, $s_2 = s_3 = r_n + \frac{D}{2}$, and $s_4 = r_{n+1}$. This Runge-Kutta method can be used even if the coordinates and functions are complex.

For the continuous condition, one should repeat calculations by changing the energy E until satisfying that

$$f_F(r_m) = f_B(r_m), \quad f(r) = \frac{A(r)}{r}, \tag{A.13}$$

$$f'_F(r_m) = f'_B(r_m), \quad f'(r) = \frac{B(r)}{r} - \frac{A(r)}{r^2}, \tag{A.14}$$

at the matching point r_m, where $f_F(r)$ and $f_B(r)$ are the forward and backward solutions, respectively.

A.3 complex-scaled version

For solving the resonant state with the complex-eigen energy, $\epsilon = E - i\Gamma/2$, the complex-scaling is utilized. Thus, the above Runge-Kutta equation is modified as

$$\frac{d}{dz}\begin{pmatrix} A(z) \\ B(z) \end{pmatrix} = \begin{pmatrix} a(z) & b(z) \\ c(z) & d(z) \end{pmatrix}\begin{pmatrix} A(z) \\ B(z) \end{pmatrix}, \tag{A.15}$$

where $z = e^{i\alpha}r$.

Appendix B

Numerov method

This is the copy of Appendix A in T. OISHI's doctoral thesis [11].

Numerov provided one numerical method to solve an ordinary differential equation in which only the zeroth and the second order terms are included, such as

$$\left[\frac{d^2}{dx^2} + f(x)\right] U(x) = 0, \tag{B.1}$$

where $f(x)$ is an arbitrary source function. The solution, $U(x)$, is sampled at equidistant points $x_n, (n = 0 \sim N)$ where the distance between two sampling points is defined as a. With this method, starting from the solution values at two consecutive sampling points, namely $U_0 \equiv U(x_0)$ and $U_1 \equiv U(x_1)$, we can calculate the remaining solution values as

$$U_{n+2} = \frac{(2 - 5a^2 f_{n+1}/6)U_{n+1} - (1 + a^2 f_n)U_n}{1 + a^2 f_{n+2}/12} + \mathcal{O}(a^6), \tag{B.2}$$

where we neglect $\mathcal{O}(a^6)$. The derivation of Eq.(B.2) is based on the discrete Taylor expansion for $U(x)$ until the fifth order. Considering the two sampling points, $x_{n-1} = x_n - a$ and $x_{n+1} = x_n + a$, Taylor expansions are given as

$$\begin{aligned} U_{n+1} &\equiv U(x_n + a) \\ &= U_n + aU'_n + \frac{a^2}{2!}U''_n + \frac{a^3}{3!}U^{(3)}_n + \frac{a^4}{4!}U^{(4)}_n + \frac{a^5}{5!}U^{(5)}_n + \mathcal{O}(a^6), \qquad \text{(B.3)} \\ U_{n-1} &\equiv U(x_n - a) \\ &= U_n - aU'_n + \frac{a^2}{2!}U''_n - \frac{a^3}{3!}U^{(3)}_n + \frac{a^4}{4!}U^{(4)}_n - \frac{a^5}{5!}U^{(5)}_n + \mathcal{O}(a^6), \qquad \text{(B.4)} \end{aligned}$$

where $U^{(m)}_n \equiv d^m U(x)/dx^m|_{x=x_n}$. The sum of these two equations gives

$$U_{n-1} + U_{n+1} = 2U_n + a^2 U''_n + \frac{a^4}{12}U^{(4)}_n + \mathcal{O}(a^6). \tag{B.5}$$

Solving this equation for $a^2 U''_n$ leads to

$$-a^2 U''_n = 2U_n - U_{n-1} - U_{n+1} + \frac{a^4}{12}U^{(4)}_n + \mathcal{O}(a^6). \tag{B.6}$$

In this equation, we can replace U''_n to $-f_n U_n$ because of Eq.(B.1). Similarly, for the fourth term in the right hand side, we can use

$$U^{(4)}(x) = \frac{d^2}{dx^2}[-f(x)U(x)]. \tag{B.7}$$

The numerical definition of the second derivative is given as the second order difference quotient, that is

$$\frac{d^2}{dx^2}[-f(x)U(x)] \Rightarrow -\frac{f_{n-1}U_{n-1} - 2f_nU_n + f_{n+1}U_{n+1}}{a^2}. \tag{B.8}$$

After these replacements, Eq.(B.6) is transformed as

$$a^2 f_n U_n = 2U_n - U_{n-1} - U_{n+1} - \frac{a^4}{12}\frac{f_{n-1}U_{n-1} - 2f_nU_n + f_{n+1}U_{n+1}}{a^2} + \mathcal{O}(a^6). \tag{B.9}$$

Finally, we solve this equation for U_{n+1} to get

$$U_{n+1} = \frac{(2 - 5a^2 f_n/6)U_n - (1 + a^2 f_{n-1})U_{n-1}}{1 + a^2 f_{n+1}/12} + \mathcal{O}(a^6), \tag{B.10}$$

which is equivalent to Eq.(B.2).

Appendix C

Two-body scattering with spherical potential

This is the copy of Appendix D in T. OISHI's doctoral thesis [11].

Our goal here is to derive the fitting formula for the phase-shift of two-body scattering problems. For simplicity, we assume that the potential between two particles is spherical. For quantum resonances in two-body systems, one can usually solve the asymptotic waves analytically. The phase shift and its derivative can be computed by using these asymptotic waves, where it indicates the pole(s) of the S-matrix for the resonance. Even if one is interested in the scattering problem with three or more particles, it is often necessary to solve the partial two-body systems in order to, *e.g.* prepare the fine two-body interactions.

C.1 solutions in asymptotic region

Assuming the relative wave function as $\phi_{ljm}(\boldsymbol{r}, \boldsymbol{s}) = R_{lj}(r)\mathcal{Y}_{ljm}(\bar{\boldsymbol{r}}, \boldsymbol{s})$, the radial equation of this problem reads

$$\left[-\frac{\hbar^2}{2\mu}\left\{\frac{d^2}{dr^2} - \frac{l(l+1)}{r^2}\right\} + V_{lj}(r) - E\right] U_{lj}(r, E) = 0, \tag{C.1}$$

where we defined $U_{lj}(r, E) \equiv rR_{lj}(r)$ from the radial wave function. The relative energy, E, for the scattering problem satisfies

$$E > \lim_{r\to\infty} V_{lj}(r) \equiv 0. \tag{C.2}$$

The equivalent but more convenient radial equation takes the form given by

$$\left[\frac{d^2}{d\rho^2} - \frac{l(l+1)}{\rho^2} - \frac{V_{lj}(r)}{E} + 1\right] U_{lj}(\rho) = 0, \tag{C.3}$$

where $\rho \equiv kr$ defined with the relative momentum, $k(E) \equiv \sqrt{2E\mu}/\hbar$. In numerical calculations, this type of equations can be solved with, *e.g.* Numerov method explained in Chapter **??**.

To calculate the phase-shift and also other important quantities, asymptotic solutions of Eq.(C.3) are often necessary. In the following, we note these solutions for two major potentials frequently used in nuclear physics.

C.1.1 with short-range potential

Short-range potentials, including nuclear interactions, are characterized as

$$\lim_{r\to\infty} V_{lj}(r) < \mathcal{O}(r^{-2}). \tag{C.4}$$

The asymptotic condition can be satisfied at $\rho \gg 1$. A general solution in this region can be written as

$$\frac{U_{lj}(\rho)}{\rho} = C_1 j_l(\rho) + C_2 n_l(\rho), \tag{C.5}$$

with spherical Bessel and Neumann functions, such as

$$j_l(kr) \longrightarrow \frac{1}{kr}\sin\left(kr - l\frac{\pi}{2}\right), \tag{C.6}$$

$$n_l(kr) \longrightarrow \frac{-1}{kr}\cos\left(kr - l\frac{\pi}{2}\right). \tag{C.7}$$

Or equivalently, the out-going and in-coming waves can be given as

$$h_l^{(+)}(kr) \equiv j_l(kr) + in_l(kr) \longrightarrow \frac{1}{ikr}e^{i\left(kr - l\frac{\pi}{2}\right)}, \tag{C.8}$$

$$h_l^{(-)}(kr) \equiv j_l(kr) - in_l(kr) \longrightarrow \frac{-1}{ikr}e^{-i\left(kr - l\frac{\pi}{2}\right)}. \tag{C.9}$$

Using the coefficients A_{lj} and B_{lj}, a general solution takes the form of

$$\begin{aligned}\frac{U_{lj}(kr)}{kr} &= A_{lj}(E)h_l^{(+)}(kr) + B_{lj}(E)h_l^{(-)}(kr) \\ &= B_{lj}(E)[S_{lj}(E)h_l^{(+)}(kr) + h_l^{(-)}(kr)],\end{aligned} \tag{C.10}$$

with the S-matrix, $S_{lj}(E) \equiv A_{lj}(E)/B_{lj}(E)$. Note that $|S_{lj}(E)|^2 = 1$ from the conservation law of the flux. Introducing the phase-shift, $\delta_{lj}(E)$ as $S_{lj}(E) \equiv e^{2i\delta_{lj}(E)}$, we can get the well-known asymptotic form of U_{lj}.

$$\begin{aligned}\frac{U_{lj}(kr)}{kr} &\longrightarrow \frac{B_{lj}(E)}{ikr}\left[S_{lj}(E)e^{i\left(kr - l\frac{\pi}{2}\right)} - e^{-i\left(kr - l\frac{\pi}{2}\right)}\right] \\ &= \frac{B_{lj}(E)e^{i\delta_{lj}(E)}}{ikr}\left[e^{i\left(kr - l\frac{\pi}{2} + \delta_{lj}(E)\right)} - e^{-i\left(kr - l\frac{\pi}{2} + \delta_{lj}(E)\right)}\right] \\ &\propto \frac{1}{kr}\sin\left[kr - l\frac{\pi}{2} + \delta_{lj}(E)\right].\end{aligned} \tag{C.11}$$

Note that $\delta_{lj}(E) \in \mathbb{R}$ since $|S_{lj}(E)|^2 = 1$.

C.1.2 with Coulomb potential

It is formulated as

$$V_{lj}(r) = V(r) = \alpha\hbar c\frac{Z_1 Z_2}{r}, \quad \alpha \equiv \frac{e^2}{4\pi\epsilon_0 \cdot \hbar c}. \tag{C.12}$$

Defining Sommerfeld parameter, $\eta \equiv Z_1 Z_2 \alpha\mu c/\hbar k$, Eq.(C.3) can be written as

$$\left[\frac{d^2}{d\rho^2} - \frac{l(l+1)}{\rho^2} - \frac{2\eta}{\rho} + 1\right] U_l(\rho, \eta) = 0. \tag{C.13}$$

With this Coulomb potential, the asymptotic condition can be satisfied at $\rho \gg 2\eta$. A general solution takes the form as

$$\frac{U_l(\rho,\eta)}{\rho} = C_1\frac{F_l(\rho,\eta)}{\rho} + C_2\frac{G_l(\rho,\eta)}{\rho}, \tag{C.14}$$

where F_l and G_l are the Coulomb functions [12]. Precise derivations of these functions are found in, *e.g.* textbook [13]. Their asymptotic forms read

$$\frac{1}{kr}F_l(kr,\eta) \longrightarrow \frac{1}{kr}\sin\left(kr - l\frac{\pi}{2} - \eta\ln 2kr + a_l(\eta)\right), \tag{C.15}$$

$$\frac{1}{kr}G_l(kr,\eta) \longrightarrow \frac{1}{kr}\cos\left(kr - l\frac{\pi}{2} - \eta\ln 2kr + a_l(\eta)\right), \tag{C.16}$$

with $a_l(\eta) = \arg\Gamma(l+1+i\eta)$, which is independent of kr. There is also an iterative formula for $a_l(\eta)$ as

$$a_{l+1}(\eta) = a_l(\eta) + \tan^{-1}\frac{\eta}{l+1}. \tag{C.17}$$

Eliminating these unimportant phases, the outgoing and incoming waves can be formulated as [13],

$$u_l^{(+)}(kr,\eta) \equiv e^{-ia_l(\eta)}\left[G_l(kr,\eta) + iF_l(kr,\eta)\right] \longrightarrow e^{i\left(kr - l\frac{\pi}{2} - \eta\ln 2kr\right)}, \tag{C.18}$$

$$u_l^{(-)}(kr,\eta) \equiv e^{ia_l(\eta)}\left[G_l(kr,\eta) - iF_l(kr,\eta)\right] \longrightarrow e^{-i\left(kr - l\frac{\pi}{2} - \eta\ln 2kr\right)}. \tag{C.19}$$

By using these functions, a general solution can be replaced to

$$U_{lj}(\rho,\eta) = A_{lj}(E,\eta)u_l^{(+)}(kr,\eta) + B_{lj}(E,\eta)u_l^{(-)}(kr,\eta) \tag{C.20}$$

$$\propto \left[S_{lj}(E,\eta)u_l^{(+)}(kr,\eta) + u_l^{(-)}(kr,\eta)\right], \tag{C.21}$$

where we need an additional variable, η, in two coefficients. The S-matrix, $S_{lj}(E,\eta)$, and the phase-shift, $\delta_{lj}(E,\eta)$, can be defined similarly in the case with short-range potentials. The asymptotic solution is also given as

$$U_{lj}(\rho,\eta) \longrightarrow\propto \sin\left[\rho - l\frac{\pi}{2} - \eta\ln 2\rho + \delta_{lj}(E,\eta)\right]. \tag{C.22}$$

In the following, however, we will not use Eqs.(C.11) and (C.22), although those are useful for analytic discussions.

C.2 fitting formula for phase shift

We explain how to compute the S-matrix within the numerical framework. First, we consider the position $r = R_b$ at which two particles can be separated sufficiently from each other. The radial mesh, dr, should be enough small compared with R_b. At this point, we assess the quantity q defined as

$$q(X) \equiv \frac{U_{lj}(X)}{U_{lj}(X+d)} \tag{C.23}$$

with $X \equiv k\cdot R_b$ and $d \equiv k\cdot dr$. Remember that the perturbed wave, $U_{lj}(X)$, is computed numerically. On the other hand, in the case with Coulomb potential for instance, $q(X)$ is also evaluated as

$$q(X) = \frac{S_{lj}(E,\eta)u_l^{(+)}(X,\eta) + u_l^{(-)}(X,\eta)}{S_{lj}(E,\eta)u_l^{(+)}(X+d,\eta) + u_l^{(-)}(X+d,\eta)}, \tag{C.24}$$

where $u_l^{(+)}$ and $u_l^{(-)}$ can be computed independently of U_{lj}. By solving Eq.(C.23) and Eq.(C.24) simultaneously for $S_{lj}(E,\eta)$, we can get

$$S_{lj}(E,\eta) = \frac{U_{lj}(X+d)u_l^{(-)}(X,\eta) - U_{lj}(X)u_l^{(-)}(X+d,\eta)}{U_{lj}(X)u_l^{(+)}(X+d,\eta) - U_{lj}(X+d)u_l^{(+)}(X,\eta)}, \tag{C.25}$$

and $2i\delta_{lj}(E,\eta) = \ln S_{lj}(E,\eta)$. This is the numerical formula for the S-matrix and the phase-shift. Notice that the similar formula can be derived in the case with short-range potentials.

Practically, it is well known that the phase-shift can be fitted by the Breit-Wigner distribution. That is

$$\delta_{lj}(E) = \tan^{-1}\left[\frac{\Gamma_0/2}{E_0 - E}\right] + C_{lj}(E), \tag{C.26}$$

or equivalently,

$$\frac{d\delta_{lj}(E)}{dE} = \frac{\Gamma_0/2}{\Gamma_0^2/4 + (E_0 - E)^2} + \frac{dC_{lj}(E)}{dE}, \tag{C.27}$$

where $C_{lj}(E)$ is a smooth back-ground. The central value, E_0, and width, Γ_0, correspond to the complex pole of the S-matrix, locating at $E = E_0 - i\Gamma_0/2$. Accordingly, we have got the fitting formula, which is equivalent to Eq.(**??**) in Chapter **??**.

References

[1] V. F. Weisskopf: Phys. Rev. **83** (1951) 1073.

[2] T. Oishi, K. Hagino, H. Sagawa: Phys. Rev. C **84** (2011) 057301.

[3] T. Oishi, N. Paar: Phys. Rev. C **100** (2019) 024308.

[4] J. Nameless: Nothing Review **9999** (9999) 9999. for dummy citation.

[5] E. Hairer, S. P. Nørsett, G. Wanner: *Solving Ordinary Differential Equations I* (Springer-Verlag, Berlin and Heidelberg, Germany, 1993). And references there in.

[6]

[7] P. Ring, P. Schuck: *The Nuclear Many-Body Problems* (Springer-Verlag, Berlin and Heidelberg, Germany, 1980).

[8] J. Suhonen: *From Nucleons to Nucleus: Concepts of Microscopic Nuclear Theory* (Springer-Verlag, Berlin and Heidelberg, Germany, 2007).

[9] I. Thompson, A. Barnett: Computer Physics Communications **36** (1985) 363.

[10] K. E. Atkinson: *An Introduction to Numerical Analysis (2nd ed.)* (John Wiley and Sons, Ltd, New York, 1989).

[11] T. Oishi, K. Hagino, H. Sagawa: Phys. Rev. C **90** (2014) 034303.

[12] *Handbook of Mathematical Functions with Formulas, Graphs, and Mathematical Tables*, ed. M. Abramowitz, I. A. Stegun (Dover Publications, Inc., New York, USA, 1972) 10th ed., Dover Books on Mathematics.

[13] T. Sasakawa: *SANRAN-RIRON (Scattering Theory)* (Shouka-Bou, Tokyo, 2007) 2nd ed.